Manipulating headgroups in Langmuir–Blodgett films through subphase pH variation

S. Kundu, A. Datta *, S. Hazra

Surface Physics Division, Saha Institute of Nuclear Physics, 1/AF Bidhannagar Kolkata 700064, India

Abstract

Cadmium arachidate Langmuir–Blodgett (LB) films, deposited at 'normal' ($\sim$6.5) and 'high' ($\sim$9.0) subphase pH on hydrophilic Si(0 0 1) have been studied by atomic force microscopy (AFM) and X-ray reflectivity techniques. Surface topography and electron density profiles (EDP) reveal absence of pinhole type defects in the 'high pH' LB film, but presence of ridges aligned roughly parallel to the direction of deposition. EDP of the films indicate nearly one extra Cd-ion per headgroup for 'high pH' films, suggesting clearly for the first time that more metal ions can be incorporated in LB films through subphase pH variation. Fourier transform infrared (FTIR) spectra indicate formation of bidentate bridging type headgroups consistent with one more metal ion per headgroup.
© 2005 Elsevier B.V. All rights reserved.

1. Introduction

A major part of the efforts in Langmuir–Blodgett (LB) film research has been focused on controlling the experimental parameters like surface pressure, temperature, pH of the aqueous subphase etc. during deposition, to obtain perfectly periodic LB films [1,2]. However, little effort has been made to manipulate the headgroups to increase the metal content and/or change the metal–headgroup interaction.

In order to manipulate metal–headgroup interaction in LB films, keeping perfection of periodicity intact, it is preferred to carry out the manipulation on the Langmuir monolayer from which the LB film is deposited. Again, one of the easiest methods to do this is by varying the pH of the aqueous subphase of the monolayer [3,4]. The divalent metal ions associated with the headgroups in the monolayer are known to form a lattice underneath the headgroups at the air–water interface [5], and this lattice, as well as the lattice formed by the organic part, can be changed by changing the subphase pH [6]. By changing pH of the subphase the metal–headgroup coordination can be changed from ionic or uncoordinated to bidentate chelating in monolayers of fatty acid salts [4]. These changes [4–6] are clear proofs that the metal–headgroup interaction can be tuned by subphase pH and provide a means to manipulate the headgroups, in particular, to increase their metal content. Acid to salt conversion increases with increasing pH and this conversion has been shown to saturate at pH $\approx$ 6.5–7.0, where LB films are normally deposited [7]. LB films have however, been deposited at higher subphase pH ($\approx$8.5) and atomic force microscopy (AFM) studies [8] of such films possess defect-free in-plane morphology as compared to the 'normal pH' films. The structure of such 'high pH' LB films along the growth direction has never been studied to extract the information about the headgroups and stacking of the films.

X-ray reflectivity is a technique, which can provide statistically average information of a thin film along the growth direction. In particular, it provides electron

---

* Corresponding author. Fax: +91 33 2337 4637.
  E-mail addresses: alok@lotus.saha.ernet.in, alok@surf.saha. ernet.in (A. Datta).

density profile (EDP) along the depth of the film [9]. In this communication, we utilized reciprocal space X-ray reflectivity along with the complementary real space AFM to bring out the differences in the morphology of cadmium arachidate (CdA) LB films deposited at different unbuffered pH values of the aqueous subphase. We have also used Fourier transform infrared (FTIR) spectroscopy to obtain the information regarding metal–headgroup coordination in LB films deposited from high subphase pH.

2. Experimental details

Arachidic acid ($CH_3(CH_2)_{18}$ COOH, Sigma, 99% pure) monolayers were spread from a 1 mg/ml chloroform (Aldrich, 99% pure) solution in a Langmuir trough (KSV 5000), on Milli-Q water (resistivity 18.2 MΩ-cm) containing cadmium chloride ($CdCl_2$, Loba Chemie, 99%). For normal LB deposition, pH of the water subphase containing 5×10^{-4} M $CdCl_2$ was maintained at 6.5 by sodium bicarbonate ($NaHCO_3$, Merck, 98%) and for deposition from high subphase pH, the pH of the water containing 5×10^{-5} M $CdCl_2$ was raised to 8.5–9.5 by adding sodium hydroxide (NaOH, Merck, 97%). NaOH was dissolved in the subphase water first to raise the pH and after 18 h, $CdCl_2$ was dissolved. Langmuir monolayers were spread 12 h after $CdCl_2$ addition. The monolayer was compressed at a constant rate of 2 mm/min. No buffers were used to maintain subphase pH so as to avoid introduction of extra and new molecular species in the system. The trough was calibrated initially by surface pressure-specific molecular area (π–A) isotherms measurements on arachidic acid Langmuir monolayers on pure water [10]. Surface pressure was measured with a Pt Wilhelmy plate.

Nine monolayers were deposited on hydrophilic Si(0 0 1) substrates for both 'normal pH' ($\approx$6.5) and 'high pH' ($\approx$9.0) condition. Si substrates were made hydrophilic after keeping it in a mixed solution of ammonium hydroxide (NH_4OH, Merck, 98%), hydrogen peroxide (H_2O_2, Merck, 98%) and Milli-Q water (water:NH_4OH:H_2O_2 $\sim$ 2:1:1, by volume) for 5–10 min at 100 °C. Depositions of both the films were done at π = 30 mN/m. Temperature during deposition was kept at 15 °C for 'normal pH' LB film, while for 'high pH' LB film it was done at 25 °C as, at high subphase pH, the transfer ratio was found to be poor at lower temperatures. Due to the known high viscosity of Langmuir monolayers at high subphase pH [8], depositions were carried out at a very slow rate (0.5 mm/min). Again, as there is a layer of hydrated ions beneath the headgroups of the Langmuir monolayers [5], a large drying time ($\approx$25 min) was allowed after each upstroke. Films were checked for reproducibility.

FTIR spectra of the film were collected with a spectrum GX (Perkin–Elmer) spectrometer in the attenuated total reflection (ATR) mode at a resolution of 4 cm^{-1} to obtain the information about the headgroups of the film. Surface topography of the films was collected through an AFM (Autoprobe CP, Park Scientific) in contact mode using silicon nitride cantilever (with 0.05 N/m low spring constant) and pyramidal tip [11]. Scans were performed in constant force mode over several portions of the film for different scan areas from 5×5 to 40×40 μm^2 and to minimize the damage of the organic films low force constant ($\sim$1 nN) was used. X-ray reflectivity studies of the LB films were carried out using a 18-kW rotating anode generator (Enraf Nonius, FR591) [9]. The X-ray beam was monochromatized using the (1 1 1) face of a silicon crystal and the radiation was collimated by slits having apertures of 100 and 5000 μm in and perpendicular to the scattering plane, respectively, to define the beam size and geometry as well as to select the Cu Kα1 component (wavelength λ = 0.1540562 nm).

3. Results and discussion

AFM images depicting the surface topography of the CdA LB films are shown in Fig. 1. The presence of large amount of defects in the surface of the 'normal pH' LB film is evident in Fig. 1a (30×30 μm^2 scan) and more so in Fig. 1b (5×5 μm^2 scan). Such 'pinhole' defects are characteristic features of 'normal pH' LB films and have been reported previously [1,12]. Although the pinhole defects actually grows in bilayer steps, the line profile drawn through the image (Fig. 1c) shows V-shaped holes due to the convolution with AFM tip. From the profile, it is also clear that defects are formed in each bilayer of the film and we observe defects of different size and depth due to cumulative effect. Deviation in depth from multiples of bilayer separation may be due to the low aspect ratio and/or high scanning speed of the AFM tip. The bearing ratio [13] obtained from the AFM analysis (Fig. 1d) shows that the coverage-area of the films slowly decreases with height, consistent with the increase of pinhole defects. The roughness of the film as a whole is very high and this is due to the presence of large amount of pinhole defects. The defect-free parts are very smooth ($\sim$0.6 nm), i.e., there is almost no out-of-plane fluctuation where CdA bilayers are present.

The situation is completely different for the 'high pH' LB film. No pinhole defects are visible in the topographic images irrespective of scan size (Fig. 1e and f). The surface is generally smooth, except for isolated bright patches. The line profile (Fig. 1g) drawn through the AFM image also indicates that. The bearing ratio suggests that there is almost no decrease in the cover-
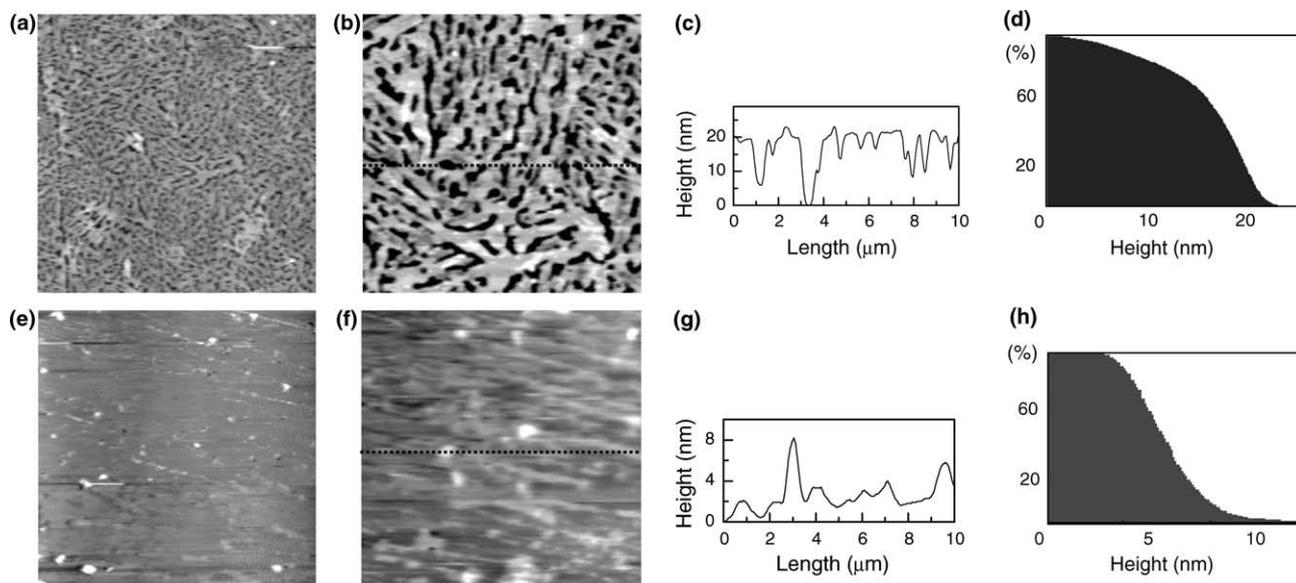
Fig. 1. AFM images and derived data of 9 ML CdA LB films prepared from two different subphase pH on silicon substrates: (a)–(d) for 'normal pH' (≈6.5) and (e)–(h) for 'high pH' (≈9.0). (a) and (e) AFM images of scan area 30 μm × 30 μm; (b) and (f) AFM images of scan area 10 μm × 10 μm; (c) and (g) Line profile drawn through AFM images indicative of height variation; (d) and (h) bearing ratio obtained from AFM images indicative of area occupation at different height.

age-area of the film with height, except on the top due to isolated patches. The roughness of the film estimated is low (~1.2 nm), similar to that observed previously [8]. However, there are undulations or ridges on the top surfaces. This is not surprising since the exact condition of film preparation, especially the time for pH stabilization, has not been stated in Ref. [12] and our conditions of deposition may differ in details. The value of roughness in the 'high pH' LB film is high when compared with the defect-free parts of the 'normal pH' LB film. This indicates, apart from the isolated patches, out-of-plane fluctuation of CdA bilayers is more in the 'high pH' LB film.

X-ray reflectivity data of 'normal pH' CdA LB film is shown in Fig. 2a. The appearance of Bragg peaks in this figure are due to the bilayer separation (d_{BL}), i.e., separation between two head-groups in the out-of-plane direction whereas the Kiessig fringes are due to the total film thickness. Up to 15 Bragg peaks are observed in this film, indicating excellent quality of the multilayer deposition. X-ray reflectivity data of 'high pH' CdA LB film is shown in Fig. 2b. Up to nine Bragg peaks clear and strong Kiessig fringes are present in this figure, which also indicate very good quality LB film. However fast decay of Bragg-peaks in the 'high pH' LB film compared to that of the 'normal pH' LB film suggests a higher interfacial roughness in the former. When the reflectivity data of both the films are plotted in same Fig. 3, the enhancement of Bragg peaks in the 'high pH' film over 'normal pH' LB film is evident in the initial part, which indicates presence of more scatterers in the head group of the former. The value of enhancement is about 2
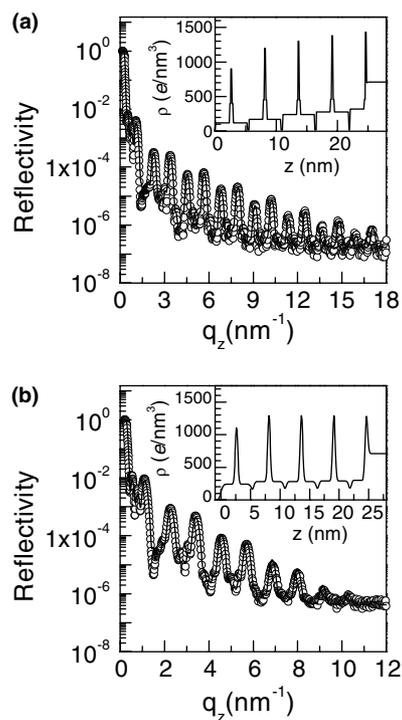
Fig. 2. (a) X-ray reflectivity data and fitted curve of 9 ML CdA LB films: (a) 'normal pH' and (b) 'high pH'. Inset: corresponding electron density profile, where air is at $z = 0$.

(from 2.78 to 1.44) on the average and nearly the same value of enhancement in the reflectivity is observed for this 'high pH' LB film when compared with the reflectivity of 'normal pH' LB film taken by other groups [14].
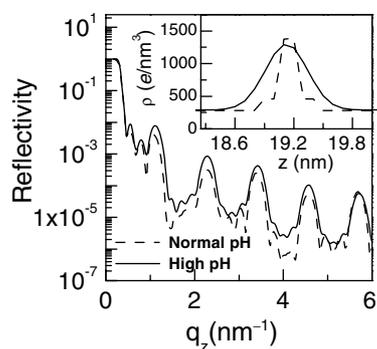
Fig. 3. Comparison between X-ray reflectivity data (selected portion) and electron density profile around the third headgroup (inset) of two 9 ML CdA LB films.

To extract quantitative information, reflectivity data of both the films have been analyzed using Parratt formalism [15]. Recursive Parratt formalism [9,15,16] for ideally flat surface/interface has however, been modified with a Debye–Waller like factor [17] for rough interface. For the analysis, films have been divided into a number of layers, each layer having a fixed thickness (d), electron density (ρ) and roughness (σ). For simplicity, each film has been divided initially into five layers, one layer containing head (d_H, ρ_H) and tail (d_T, ρ_T) just above substrate and four bilayers of same thickness (d_{BL}) above that. Each bilayer consists of one tail each on two sides and head in the middle. In addition, we have considered same interfacial roughness (σ_{if}) throughout a film, except in the top (σ_t) and the bottom (σ_b). A thin layer of negligible density has been inserted between two hydrocarbon tail layers due to the presence of hydrogen atoms of methyl group at the end of tail chain [18,19]. Data of both the films are then fitted by the analysis scheme outlined above with the d's, ρ's and σ's as fitting parameters [9,15,16]. The calculated reflectivity curves are shown in the Fig. 2a and b by solid lines and the corresponding EDPs of the film are shown in the inset.

The EDP of the 'normal pH' LB film shows that the coverage decreases with increasing layer number (upwards) from the silicon surface as the electron density decreases with increasing film thickness. Although the interface width is negligible, the 'pinhole' defects reduce the layer coverage, giving rise to a slowly decreasing EDP, which is consistent with AFM line profiles. The reflectivity data has been fitted up to 15 orders of Bragg peaks along with the Kiessig (interference) fringes to obtain the accurate EDP of the film. The resolution with which the strong Bragg peaks and small Kiessig fringes can be fitted is $\pi/q_{z,max}$ [20], i.e., with ~0.17 nm for this very high quality reflectivity data. For getting information about the 0.6 nm thick headgroup at the highest resolution allowed by the data we have divided the headgroups into three layers of thickness 0.2 nm each. The

EDP shows that the middle layer of each headgroup has $\rho \sim 1250$ electrons per nm^3, while the upper and lower layers have density around 440 electrons per nm^3. As the latter corresponds closely to the electron density of the carboxyl (COO^-) group, the former can be assigned to the Cd-ion (atom).

The EDP of the 'high pH' LB film shows that the coverage is not decreasing with increasing layer number, as it remains nearly constant up to three and half bilayer. Only in the upper bilayer the electron density is less which matches very well with the AFM results as bearing ratio starts to decrease nearly after three bilayer distance from the top of the silicon substrate. Reflected intensity falls off quite slowly and this could be fitted with a conformal interface of width 0.195 nm. The resolution with which the data is fitted is ~0.26 nm. The metal-bearing part of the 0.6 nm thick headgroup is ~0.3 nm thick and the average electron density of this part is 2100 electrons per nm^3 consistent with higher Cd-accumulation.

To have better understanding of these headgroups, we have performed a preliminary calculation for the number of electrons for each of these headgroups. Assuming a cross-sectional area of ~0.18 nm^2 per hydrocarbon chain [1], and a symmetric arrangement of tails about the headgroup as are seen in CdA LB films [21], we considered the cross-sectional area of headgroup to be 0.18 nm^2 too. In the previous study in 'high pH' LB films [8] no major change in this area was noted. If we integrate around the same range (z value) of a particular headgroup from the electron density profile and then multiply this integrated value with the cross-sectional value of the headgroup we obtain the number of electrons that is incorporated within the headgroups. For example, we have taken the second headgroup layer from the (bottom) silicon surface where coverage is nearly unity for both types of films. The EDPs for this headgroup in the two films are shown in the inset of Fig. 3 for comparison. The integrated values obtained from the EDPs of the two different LB films ('normal' and 'high' pH) for the same length around the second headgroups are 698.0 and 927.0 electrons per nm^2, respectively. Multiplying these values with the cross-sectional area, we obtain the number of electrons within the headgroups to be 126 and 167 for 'normal' and 'high' pH LB films. The number difference of electrons is 41, closely matching the number of electrons in one cadmium atom (48). Bilayer separation is 5.5 and 5.52 nm for 'normal' and 'high' pH LB films, i.e., there is no increase in either the head or the tail thicknesses for the 'high pH' LB film. However, the interfaces become comparatively rough. This implies that the extra cadmium ion (atom) is incorporated in the xy-plane with fluctuation in the out-of-plane direction. This out-of-plane fluctuation is manifested on the top of the 'high pH' LB films as observed from AFM analysis.

FTIR spectra of the 'high pH' LB film were studied to understand the metal–headgroup coordination that can account for this excess in cadmium. Metal–carboxylate complexes introduce a shift in the positions of the asymmetric (v_a) and symmetric (v_s) stretch modes of the COO^- group from the free carboxylate ion values. The carboxylate ion may coordinate to a metal ion in three ways: unidentate coordation, bidentate chelating coordation and bidentate bridging coordation [22]. In the unidentate complex the gap (Δ) between the symmetric and asymmetric modes is much larger than in the free ion. The opposite trend is observed in the bidentate chelating complex where the Δ is smaller than that of the free ion [4]. In the bidentate bridging complex, however, Δ is nearly same as observed in free ion but the positions are shifted according to specific metal ions [22]. In FTIR spectra of 'high pH' LB film as shown in Fig. 4 the observed broad peak at 1585 cm^{-1} is due to v_a. If the peaks observed at 1447 and at 1466 cm^{-1} are considered due to the asymmetrical bending vibrations of the methyl group (δ_a) and scissoring band of the methylene group (δ_s) then one of the remaining peaks observed at 1454, 1458 and 1462 cm^{-1} must be due to the v_s. Hence, the separations Δ are 131, 127 and 123 cm^{-1}, respectively. It is to be noted that Δ for the free carboxylate ions is reduced with increasing hydrocarbon groups [22] and the available observed value of $\Delta = 144$ cm^{-1} is for free acetate ions. Hence, our observed Δ for the headgroup–metal complex in the 'high pH' LB films is nearly same as free ion with a metal induced shift in the peak positions. This implies that the metal carboxylates are in the bidentate bridging mode. The model structure of headgroup is shown in the inset of Fig. 4. This bidentate bridging coordination of the metal–headgroup complex in 'high pH' LB film matches with the one extra cadmium ion per headgroup obtained from X-ray reflectivity analysis.
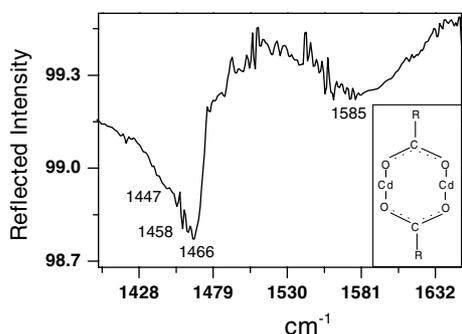
Fig. 4. FTIR spectra in the ATR mode of 9 ML CdA 'high pH' LB film. Absorbance peaks at different wave numbers (cm^{-1}) are explained in the literature. Inset: bidentate bridging type headgroup model formed in 9 ML CdA 'high pH' LB film. R is for hydrocarbon chain of fatty acid.

4. Conclusions and outlook

Fig. 5 summarizes, in cartoon form, the results of our studies on the (to our knowledge) first successful incorporation of extra metal ions in the metal-bearing headgroups of LB multilayers with little impairment to the periodicity, interfacial width and top roughness of the multilayer stack. We have manipulated the headgroups by raising the pH (to ≈ 9.0) of the aqueous subphase of the Langmuir monolayer from which the multilayer was deposited on Si(0 0 1) substrates. For comparison, we have deposited a LB multilayer under identical condition but with the subphase pH in the 'normal' (≈ 6.5) range. We have studied both types of LB multilayers with contact-mode AFM and X-ray reflectivity.

The 'normal pH' LB multilayer (Fig. 5a), as confirmed by both studies, is dominated by pinhole defects in its growth (Fig. 5b) the holes starting from nearly the bottom layer and becoming wider as they go to the top, thereby reducing the coverage and density in subsequent upward layers (Fig. 5a and b). However, X-ray scattering studies show that the cadmium ions in the headgroups are confined within sharp interfaces (Fig. 5c), which again is reflected in the AFM by the low top roughness in the regions between pinholes (Fig. 5b). Detailed X-ray analysis shows that there is one cadmium ion between two carboxylic (COO^-) groups in each headgroup (Fig. 5d). The bilayer separation (d_{BL}) is consistent with untilted chains of $CH_3(CH_2)_{18}$, the hydrocarbon 'tail' of arachidic acid.

The 'high pH' LB multilayer, shown in Fig. 5e has very few pinhole defects, and the few that are there, are confined to the top layer (Fig. 5f). Hence, there is almost no variation in coverage or density with depth and the coverage is nearly unity throughout (Fig. 5e and f). On the other hand, the cadmium ions in the headgroups are confined within interfaces that have larger width or roughness (Fig. 5g) giving rise to undulations or ridges on the top of the film through conformality (Fig. 5f). The presence of two cadmium-ions with one COO^- group on either side in the headgroup has been confirmed from detailed analysis of X-ray data (Fig. 5h). Analysis FTIR data indicates a bidentate bridging type coordination of cadmium ions to headgroups. This is also consistent with the existence of one more metal ion per each headgroup. The extra metal ion in each headgroup of the multilayer leads to a near twofold increase in its X-ray reflectivity. The bilayer separation here is almost the same as in the 'normal' multilayer.

As the headgroups of the LB films deposited from 'high' subphase pH have nearly the same thickness as 'normal' headgroups so metal ions are incorporated in the xy-plane, i.e., in the plane of the headgroups and a structural study such as grazing incidence diffraction (GID) can elucidate these novel structure and correlate them with results of GID studies on Langmuir
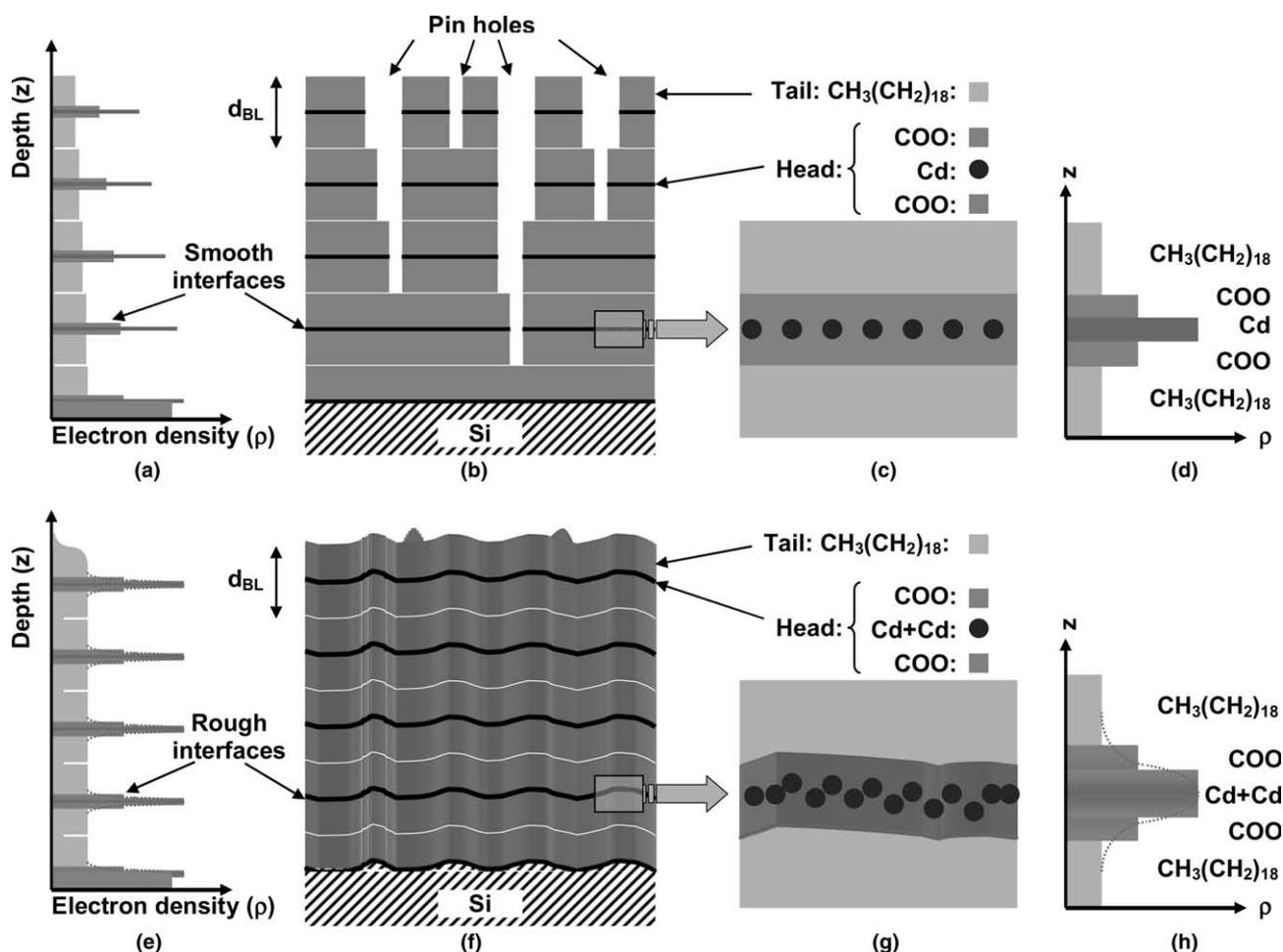
Fig. 5. Model morphology of 9 ML CdA LB films prepared from two different subphase pH on silicon substrates: (a)–(d) for 'normal pH' and (e)–(h) for 'high pH'. (a) and (e) Electron density profile; (b) and (f) cross-sectional view with pin-hole defects of different height and size; and smooth interfaces in the 'normal pH' LB film, while some patches on the top and rough interfaces in the 'high pH' LB film; (c) and (g) cross-sectional view of selected portion with compositional profile of head and tail; (d) and (h) electron density profile of selected portion.

monolayers. Although the manipulation of headgroups by incorporating metal ions and its deposition on some solid substrate has been successful, nevertheless work is underway for obtaining better films with lower interfacial width for obtaining higher reflectivity up to higher orders of Bragg peaks.

References

[1] D.K. Schwartz, Surf. Sci. Rep. 27 (1997) 245.
[2] J. Als-Nielsen, D. Jacquemain, K. Kjaer, F. Leveiller, M. Lahav, L. Leiserowitz, Phys. Rep. 246 (1994) 251.
[3] F. Leveiller, C. Böhm, D. Jacquemain, H. Möhwald, L. Leiserowitz, K. Kjaer, J. Als-Nielsen, J. Phys. Chem. 96 (1992) 10380.
[4] Y. Ren, K.-i. Iimura, T. Kato, Langmuir 17 (2001) 2688.
[5] J. Kmetko, A. Datta, G. Evmenenko, P. Dutta, J. Phys. Chem. B 105 (2001) 10818.
[6] A. Datta, J. Kmetko, C.J. Yu, A.G. Richter, K.S. Chung, J.M. Bai, P. Dutta, J. Phys. Chem. B 104 (2000) 5797.
[7] J.M. Bloch, W. Yun, Phys. Rev. A 41 (1990) 844.
[8] D.Y. Takamoto, E. Aydil, J.A. Zasadzinski, A.T. Ivanova, D.K. Schwartz, T. Yang, P.S. Cremer, Science 293 (2001) 1292.
[9] M.K. Sanyal, A. Datta, S. Hazra, Pure Appl. Chem. 74 (2002) 1553.
[10] V.M. Kaganer, H. Möhwald, P. Dutta, Rev. Mod. Phys. 71 (1999) 779.
[11] J.K. Basu, S. Hazra, M.K. Sanyal, Phys. Rev. Lett. 82 (1999) 4675.
[12] Th. Geue, M. Schultz, U. Englisch, R. Stömmer, U. Pietsch, J. Chem. Phys. 110 (1999) 8104.
[13] S. Kundu, S. Hazra, S. Banerjee, M.K. Sanyal, S.K. Mandal, S. Chaudhuri, A.K. Pal, J. Phys. D: Appl. Phys. 31 (1998) L73.
[14] V. Nitz, M. Tolan, J.-P. Schlomka, O.H. Seeck, J. Stettner, W. Press, Phys. Rev. B 54 (1996) 5038.
[15] L.G. Parratt, Phys. Rev. 95 (1954) 359.
[16] M. Tolan, X-Ray Scattering from Soft Matter Thin Films, Springer, Berlin, 1999.
[17] M. Piecuch, L. Nevot, Mater. Sci. Forum 59–60 (1990) 93.
[18] A. Gibaud, S. Hazra, Curr. Sci. 78 (2000) 1467.
[19] A.I. Kitaigorodskii, Organic Chemical Crystallography, Consultant Bureau, New York, 1961.
[20] J. Daillant, M. Alba, Rep. Prog. Phys. 63 (2000) 1725.
[21] M.K. Sanyal, M.K. Mukhopadhyay, M. Mukherjee, A. Datta, J.K. Basu, J. Penfold, Phys. Rev. B 65 (2002) 033409.
[22] K. Nakamoto, Infrared and Raman Spectra of Inorganic and Coordination Compounds, Wiley, New York, 1986.